SNX18 shares a redundant role with SNX9 and modulates endocytic trafficking at the plasma membrane

Joohyun Park[1,*], Yoonju Kim[1,2,*], Suho Lee[1,2], Jae Jun Park[2], Zee Yong Park[2], Woong Sun[3], Hyun Kim[3] and Sunghoe Chang[1,2,‡]

[1]Department of Biomedical Sciences, Seoul National University, College of Medicine, Seoul 110-799, South Korea
[2]Department of Life Science, Gwangju Institute of Science and Technology, Gwangju 500-712, South Korea
[3]Department of Anatomy, Korea University, College of Medicine, Sungbuk-Gu, Seoul 136-705, South Korea
*These authors contributed equally to this work
‡Author for correspondence (sunghoe@snu.ac.kr)

Accepted 22 February 2010
Journal of Cell Science 123, 1742-1750

doi:10.1242/jcs.064170

Summary

SNX18 and SNX9 are members of a subfamily of SNX (sorting nexin) proteins with the same domain structure. Although a recent report showed that SNX18 and SNX9 localize differently in cells and appear to function in different trafficking pathways, concrete evidence regarding whether they act together or separately in intracellular trafficking is still lacking. Here, we show that SNX18 has a similar role to SNX9 in endocytic trafficking at the plasma membrane, rather than having a distinct role. SNX18 and SNX9 are expressed together in most cell lines, but to a different extent. Like SNX9, SNX18 interacts with dynamin and stimulates the basal GTPase activity of dynamin. It also interacts with neuronal Wiskott-Aldrich syndrome protein (N-WASP) and synaptojanin, as does SNX9. SNX18 and SNX9 can form a heterodimer and colocalize in tubular membrane structures. Depletion of SNX18 by small hairpin RNA inhibited transferrin uptake. SNX18 successfully compensates for SNX9 deficiency during clathrin-mediated endocytosis and vice versa. Total internal reflection fluorescence microscopy in living cells shows that a transient burst of SNX18 recruitment to clathrin-coated pits coincides spatiotemporally with a burst of dynamin and SNX9. Taken together, our results suggest that SNX18 functions with SNX9 in multiple pathways of endocytosis at the plasma membrane and that they are functionally redundant.

Key words: SNX18, SNX9, Clathrin-mediated endocytosis, Dynamin, Membrane tubulation

Introduction

Endocytic pathways take membrane receptors and extracellular components into the cell, leading to activation of intracellular signaling pathways. Although several distinct endocytic pathways are known, clathrin-mediated endocytosis is the best characterized. Clathrin-mediated endocytosis begins by gathering membrane proteins and lipids through interactions with cytosolic adaptors and accessory factors, which bind to clathrin and initiate polymerization of triskeletal clathrin molecules into a spherical basket of clathrin-coated pits (CCPs) (Schmid et al., 2006; Schmid and McMahon, 2007). Subsequently, the accessory proteins, such as amphiphysin, endophilin and sorting nexin 9 (SNX9), are concentrated at the membrane, inducing membrane curvature and the formation of intermediate tubular membrane structures (Farsad et al., 2001; Masuda et al., 2006; Peter et al., 2004; Shin et al., 2008; Takei et al., 1999). Finally, dynamin cuts off the tubular necks and releases the clathrin-coated vesicle into the cytoplasm (Itoh et al., 2005; Praefcke and McMahon, 2004; Roux et al., 2006). Proteins with membrane tubulating activity commonly have a Bin-amphiphysin-Rvs (BAR) domain and a Src homology 3 (SH3) domain (Dawson et al., 2006; Farsad and De Camilli, 2003; Itoh and De Camilli, 2006; Tsujita et al., 2006). Recent crystal structures of the BAR domains of amphiphysin and endophilin revealed that the BAR domain forms a banana-shaped dimer that deforms the membrane to form tubular structures in vitro and in vivo (Habermann, 2004; Peter et al., 2004; Weissenhorn, 2005). The SH3 domain is involved in interactions with endocytic proteins and actin regulatory proteins such as dynamin and synaptojanin (Evergren et al., 2007; Hill et al., 2001; Kim et al., 2005; Soulet et al., 2005).

Dynamin plays a crucial role in clathrin-mediated endocytosis (Hinshaw, 2000). Its N-terminal domain is responsible for GTP hydrolysis and its C-terminal proline-rich domain (PRD) links it to SH3-domain-containing proteins such as amphiphysin, endophilin and SNX9. The central pleckstrin homology (PH) domain controls the binding of dynamin to membrane phospholipids (Klein et al., 1998). A coiled-coil domain (also called the GTPase effector domain or GED) that follows the PHD might play an important role in dynamin self-assembly and regulation of GTPase activity. There are three known isoforms of dynamin in mammals. Dynamin-1 is dominantly expressed in neuronal cells and contributes to synaptic-vesicle recycling (Nakata et al., 1991; Shpetner and Vallee, 1989). Dynamin-2 is expressed ubiquitously and its function is similar to that of dynamin-1 (Altschuler et al., 1998; Damke et al., 1994). Dynamin-3 is expressed in testis, but its function is still not well understood (Gray et al., 2003).

Recently, evidence has shown that SNX9 plays a key role in clathrin-mediated endocytosis (Lundmark and Carlsson, 2003; Lundmark and Carlsson, 2009; Shin et al., 2008; Soulet et al., 2005; Yarar et al., 2008). SNX9 forms a complex with dynamin in the cytosol and regulates the recruitment of dynamin to the membrane (Lundmark and Carlsson, 2002). Furthermore, SNX9 enhances dynamin assembly and increases its GTPase activity (Soulet et al., 2005). Other endocytic molecules and actin regulatory proteins, adaptor protein complex 2 (AP-2), the Arp2/3 complex

and clathrin also bind to the low-complexity (LC) region of SNX9 in a cooperative manner (Lundmark and Carlsson, 2003; Lundmark and Carlsson, 2009; Shin et al., 2008). The SNX family contains two proteins that are closely related to SNX9: SNX18 and SNX33. All three have the same domain structure. An SH3 domain at the N terminus is followed by an LC domain of variable length, with a Phox homology (PX)-BAR region at the C terminus. It has been suggested that SNX18 and SNX33 branched off from SNX9, and were then duplicated (Haberg et al., 2008). Because SNX9 has a crucial role in clathrin-mediated endocytosis, it is of interest to also investigate the expression and function of SNX18 and SNX33.

A recent paper showed that SNX9, SNX18 and SNX33 localize differently in cells and appear to function in different trafficking pathways (Haberg et al., 2008). Whereas SNX9 localizes to plasma-membrane endocytic sites, SNX18 is found on peripheral endosomal structures. The LC domain of SNX18 contains a binding motif for adaptor protein complex 1 (AP-1) and it colocalizes with PACS1, but not with clathrin. SNX18 functions in an endosomal trafficking pathway that does not rely on clathrin, but is dependent on AP-1 and the retrograde trafficking protein PACS1 (Haberg et al., 2008).

Here, however, we show that SNX18 and SNX9 are functionally redundant, and that SNX18 has a similar role to SNX9 in clathrin-mediated endocytosis, rather than a distinct role in endosomal trafficking. SNX18 and SNX9 are expressed together in most cell lines, but to a different extent. For example, SNX9 is dominantly expressed in HeLa cells and COS-7 cells, whereas SNX18 is dominantly expressed in the C6 glioma cell line. SNX18 interacts with dynamin, neuronal Wiskott-Aldrich syndrome protein (N-WASP) and synaptojanin – well-known binding partners of SNX9. SNX18 stimulates the basal GTPase activity of dynamin and regulates its recruitment to the plasma membrane. SNX18 can form homodimers and heterodimers with SNX9, and they colocalize in tubular membrane structures when overexpressed. Unlike the previous report (Haberg et al., 2008), we could not detect any colocalization of SNX18 with AP-1 or a cation-independent mannose-6-phosphate receptor (CI-MPR). SNX18 colocalizes with neither 2xPH (FAPP1), a *trans*-Golgi marker, nor 2xFYVE (Hrs), an endosome marker. Instead, it colocalizes with clathrin and dynamin at the plasma membrane. In addition, SNX18 successfully replaced SNX9, such that defects in transferrin internalization caused by the depletion of SNX9 in HeLa cells are recovered by compensatory expression of SNX18 and vice versa. Depletion of SNX18 in C6 glioma cells caused endocytic defects. Using total internal reflection fluorescence (TIRF) microscopy in living cells, we detected a transient burst of SNX18 recruitment to CCPs that coincides spatially and temporally with a burst of RFP-dynamin fluorescence and with a burst of SNX9; this occurs concomitantly with the disappearance of clathrin fluorescence. Taken together, our results suggest that SNX18 functions in multiple endocytic trafficking pathways at the plasma membrane, rather than in a distinct endosomal trafficking pathway, and that SNX18 and SNX9 are functionally redundant.

Results

Expression of SNX18 in various cell lines and during development

To assess the cellular distribution of SNX18, an antibody was raised against recombinant SNX18 (supplementary material Figs S1, S2). Immunoblotting analysis was carried out in different cell lines from different species to compare its distribution with that of SNX9. Most cell lines expressed both proteins, but to a different extent. SNX9 was dominantly expressed in HeLa, TM4, L929 and COS-7 cells, whereas SNX18 was more strongly expressed than SNX9 in C6, Ha-CAT, HL-1 and NIH-3T3 cells (Fig. 1B).

To investigate the tissue distribution of SNX18 during development, the expression of *SNX18* mRNA was examined by in situ hybridization with parasagittal sections of whole embryos (E16 and E18) or coronal sections of postnatal mouse brains (P3, P7 and adult) (Fig. 1C). SNX18 is widely expressed in the developing embryos. On E16, *SNX18* mRNA signals were found throughout the CNS and various peripheral tissues, including liver,

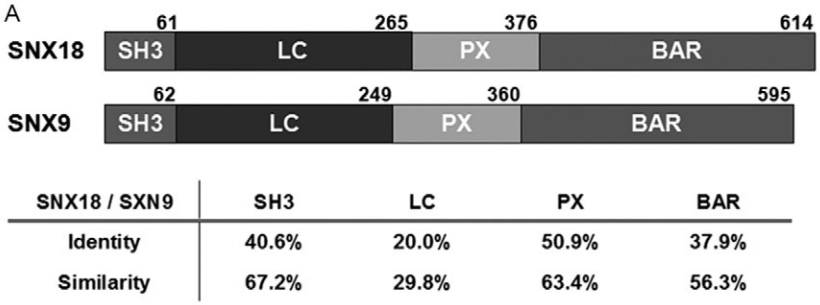

SNX18 / SXN9	SH3	LC	PX	BAR
Identity	40.6%	20.0%	50.9%	37.9%
Similarity	67.2%	29.8%	63.4%	56.3%

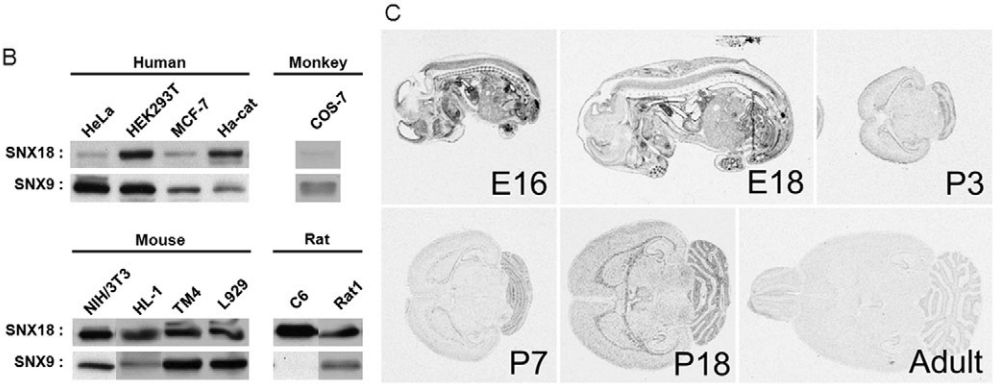

Fig. 1. Expression patterns of SNX18 in various cell lines and during development. (**A**) Schematic diagrams of SNX18 and SNX9 and their domain structures. Individual domain sequences were aligned with ClustalW software. (**B**) Immunoblotting analysis of different cell lines from different species using anti-SNX18 and anti-SNX9 antibodies. The same amount of protein was loaded in each lane. (**C**) In situ hybridization with parasagittal sections of whole embryos (E16 and E18) or coronal sections of postnatal mouse brains (P3, P7 and adult). Scale bar: 5.0 μm.

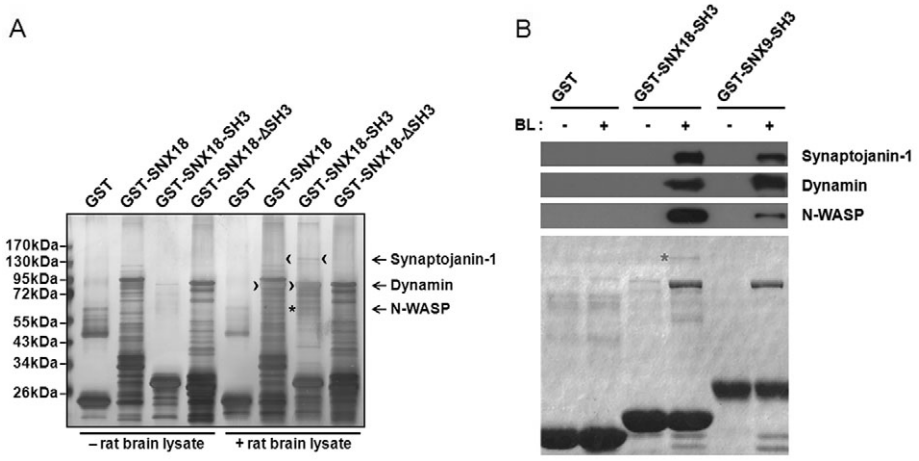

Fig. 2. SNX18 interacts with dynamin, N-WASP and synaptojanin. (**A**) Rat brain lysates were incubated with GST, GST-SNX18, GST-SNX18-SH3 and GST-SNX18-ΔSH3. SDS-polyacrylamide gels were stained with silver. Specific bands were excised from the stained gel, and analyzed by micro-LC-MS/MS and by a protein database search, identifying synaptojanin (<), dynamin (>) and N-WASP (*). (**B**) GST fusion proteins of SNX18-SH3 and SNX9-SH3, and GST alone were incubated with rat brain lysates (BL) and SDS-polyacrylamide gels were stained with Coomassie Brilliant Blue. The proteins were transferred to a polyvinylidine difluoride membrane and immunoblotted with anti-synaptojanin antibody, anti-dynamin-1 antibody or anti-N-WASP antibody. The asterisk indicates the band including synaptojanin-1.

lung, heart, thymus and intestine. On E18, the expression of SNX18 was decreased compared with that on E16. On P3, SNX18 expression was found in the outer layer of the cerebral cortex, hippocampal formation, external germinal layer of the cerebellum and internal capsule. Similar expression patterns were maintained on P7-P18. At these stages, *SNX18* mRNA was found in the external germinal layer (P7) and granular layer (P18) of the cerebellum. In addition, the mRNA signal was also prominent in the external capsule. In the adult mouse brain, substantial expression of *SNX18* mRNA was observed in the hippocampal formation and cerebellum. In addition, moderate levels of signal were found in the glomerular layer of the olfactory bulb.

SNX18 interacts with dynamin, N-WASP and synaptojanin

Because SNX18 contains an SH3 domain and its SH3 domain is similar to that of SNX9, it could bind PRD-containing proteins. To identify proteins that interact with the SH3 domain of SNX18, we carried out a series of GST pull-down assays and performed a micro-LC-MS/MS analysis (Fig. 2A). Brain lysates were pulled down with GST-SNX18, GST-SH3-SNX18 and GST-ΔSH3-SNX18, and SDS-polyacrylamide gels were silver stained. After in-gel digestion, micro-LC-MS/MS and a protein database search identified dynamin, N-WASP and synaptojanin (Fig. 2A). GST pull-down assays followed by immunoblotting with specific antibodies further confirmed that SNX18 interacts with dynamin, synaptojanin-1 and N-WASP (Fig. 2B), as does SNX9 (Shin et al., 2007; Yarar et al., 2008).

SNX18 stimulates the basal GTPase activity of dynamin and its recruitment to the plasma membrane

SNX9 binds to dynamin and stimulates its basal GTPase activity (Soulet et al., 2005). To determine whether the interaction of SNX18 and dynamin regulates aspects of dynamin activity, we have measured the basal rate of GTP hydrolysis of dynamin in the presence of GST-SNX18. Fig. 3A shows that GST-SNX18 stimulated the basal GTPase activity of dynamin-1; this is fully comparable to the action of GST-SNX9.

To see whether SNX18 affects the localization of dynamin, C6 glioma cells (where SNX18 is dominantly expressed and SNX9 is almost absent; see Fig. 1B) were co-transfected with dynamin-2–GFP and either *SNX18* short hairpin RNA (shRNA) or mock vector. TIRF imaging was then performed. We found that the membrane recruitment of dynamin-2 was significantly lower in SNX18 knock-down cells compared with control cells (Fig. 3B,C). This is consistent with the previous report regarding the role of SNX9 in dynamin localization (Lundmark and Carlsson, 2004).

SNX18 and SNX9 form a heterodimer, and are colocalized on membrane tubules when overexpressed

SNX18 contains a BAR domain, suggesting that it can dimerize and oligomerize. Indeed, SNX18 homodimerizes and

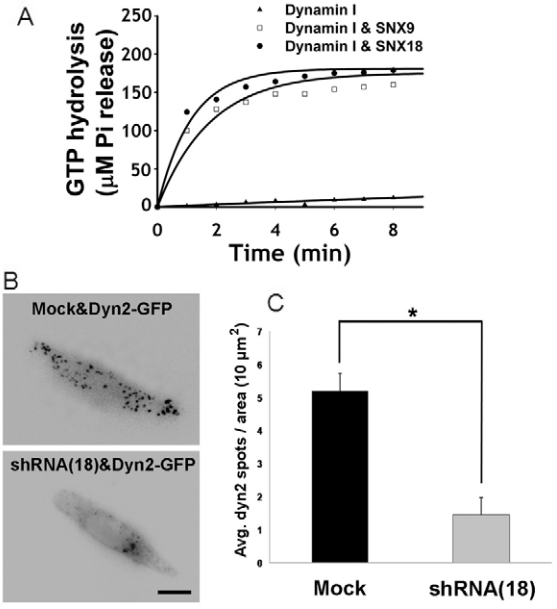

Fig. 3. SNX18 stimulates the basal GTPase activity of dynamin and its recruitment to the plasma membrane. (**A**) Basal dynamin-1 GTPase activity was measured using the GTPase ELIPA assay. 1 μM dynamin I was mixed with 1 μM GST-SNX18 or GST-SNX9, and added to prepared ELIPA mixture with 1 mM GTP. The amount of inorganic phosphate released by dynamin-1 only or in the presence of GST-SNX18 or GST-SNX9 was measured at 360 nm with 1 minute intervals and plotted as a function of time. (**B**) TIRF microscopy images of C6 glioma cells transfected with dynamin 2-GFP and mock, or SNX18 shRNA. Three days after transfection, cells were imaged using TIRF microscopy. Scale bar: 10 μm. (**C**) Bar graph indicating that SNX18 depletion in C6 cells blocks the recruitment of dynamin-2 to the plasma membrane. *Statistically significant at $P<0.05$, Student's *t*-test.

heterodimerizes with SNX9 in vivo and in vitro, and does so by means of its BAR domain (Fig. 4A,B). BAR-domain-containing proteins are known to trigger membrane deformation and invagination, known to be required for the formation of intermediate structures during clathrin-mediated endocytosis (Dawson et al., 2006; Farsad and De Camilli, 2003; Habermann, 2004). When overexpressed, these proteins induce the formation of massive membrane tubules. It has been shown that SNX9 can induce membrane tubules, which requires its PX and BAR domains. SNX18 also contains PX and BAR domains and, as recently shown, SNX18 can also tubulate the plasma membrane (Fig. 4C,D). Live confocal microscopy showed that SNX18-GFP and SNX9-mRFP colocalized with each other on the tubules, rather than showing patch overlap, as has been found in a recent study (Haberg et al., 2008). This is consistent with our findings that they could form a heterodimer (Fig. 4C,D).

SNX18 localizes at the cell surface, where it is partially colocalized with clathrin and dynamin

A previous study showed that endogenous SNX18 colocalizes with AP-1 and PACS1-positive endosomal structures, which are devoid of clathrin (Haberg et al., 2008). Our immunostaining studies, however, showed that endogenous SNX18 colocalizes neither with AP-1, a late endosome marker (Fig. 5A-D), nor with CI-MPR, a *trans*-Golgi marker (supplementary material Fig. S3). TIRF microscopy was used to visualize the proteins in the vicinity of the plasma membrane and clearly showed that endogenous SNX18 colocalizes not with AP-1 (Fig. 5D), but rather partially with clathrin and dynamin at the cell surface (Fig. 6A,B).

Consistent with their heterodimerization, endogenous SNX18 and SNX9 were colocalized at the cell surface as well (Fig. 6C).

When exogenously expressed, SNX18 colocalized neither with RFP-2xPH (FAPP1), a PtdIns(4)*P* marker, nor with GFP-2xFYVE (Hrs), a PtdIns(3)*P* marker, suggesting that it is not located in the Golgi complex or in early endosomes (supplementary material Fig. S4). This result is consistent with the previous report showing that SNX18 has a preference for PtdIns(4,5)P_2 lipids, which are enriched in the plasma membrane (Haberg et al., 2008).

SNX18 can replace the function of SNX9 during clathrin-mediated endocytosis

Considering the structural similarity of SNX18 and SNX9, and the fact that they share binding partners, SNX18 could have a role in clathrin-mediated endocytosis. In fact, knocking down endogenous expression of SNX18 using shRNAs inhibits transferrin uptake in C6 glioma cells, where SNX18 is dominantly expressed (Fig. 7A,B; supplementary material Fig. S5). Next, we wondered whether SNX18 could compensate for lack of SNX9 during clathrin-mediated endocytosis and vice versa. We overexpressed SNX18 or SNX9 in a SNX9 or SNX18 knock-down background, respectively.

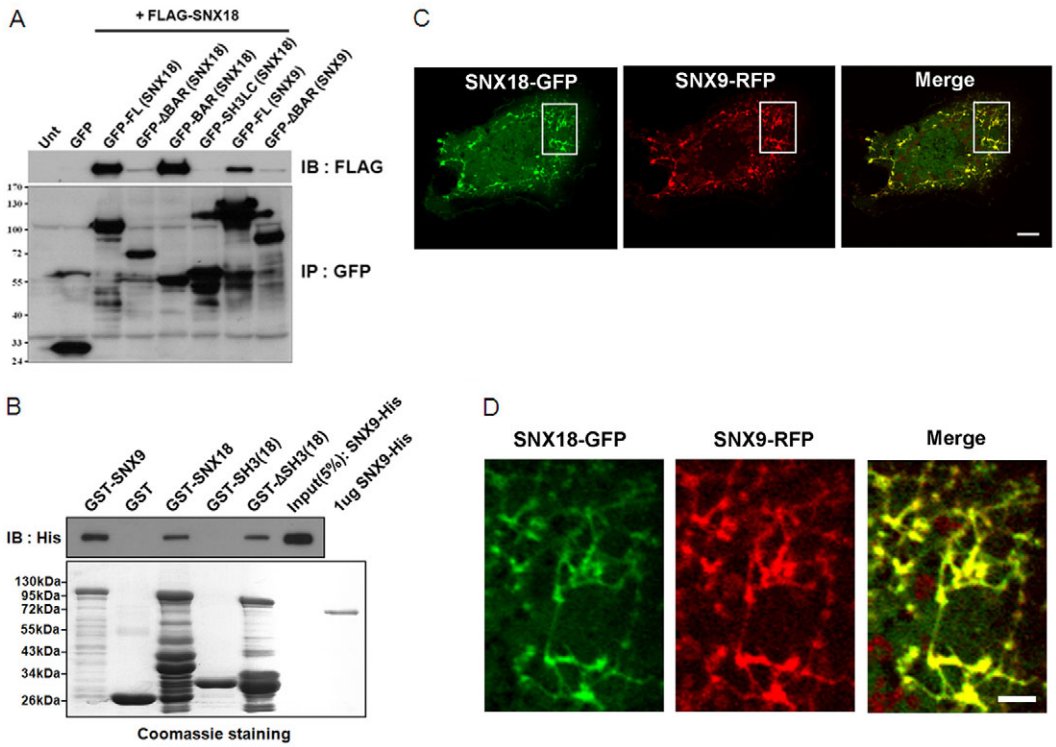

Fig. 4. SNX18 and SNX9 form a heterodimer, and are colocalized on membrane tubules. (**A**) HEK293T cells were co-transfected with GFP-FL(SNX18), ΔBAR(SNX18), BAR(SNX18), SH3LC(SNX18), FL(SNX9), ΔBAR(SNX9) or GFP alone, and FLAG-SNX18. 24 hours after transfection, the cells were lysed and immunoprecipitated (IP) with anti-GFP antibody, and immunoblotted (IB) with anti-FLAG antibody. Unt, untransfected; FL, full length. (**B**) In vitro binding assays were carried out with purified SNX9-His and GST-SNX9, GST-SNX18, ΔSH3 (SNX18), SH3 (SNX18) or GST alone, followed by immunoblotting with anti-His antibody. Input(5%):SNX9-His was used as a positive control. GST-SNX9, GST-SNX18 and GST-SNX18-ΔSH3 but not GST-SNX18-SH3 bind to SNX9-His, confirming the direct interaction of SNX18 with SNX9. (**C**) COS-7 cells were transfected with SNX18-GFP and SNX9-mRFP, and time-lapse imaging was performed 14 hours after transfection. Scale bar: 10 µm. (**D**) High-magnification views of the regions in C enclosed in rectangles. SNX18-GFP and SNX9-mRFP are colocalized on the membrane tubules. Scale bar: 2 µm.

SNX9 or SNX18 knock down resulted in defective transferrin uptake in HeLa cells or C6 glioma cells, where SNX9 or SNX18 is dominantly expressed, respectively. SNX9 successfully rescued the endocytic defects caused by SNX18 depletion in C6 glioma cells (Fig. 7A,B) whereas the endocytic defects caused by SNX9 depletion in HeLa cells were rescued by cotransfection of SNX18 (Fig. 7C,D). These results suggest that SNX18 plays a similar role to SNX9 during clathrin-mediated endocytosis.

Mutants of SNX9 and SNX18 with their SH3 domain deleted (ΔSH3-SNX9 in Fig. 7A,B and ΔSH3-SNX18 in Fig. 7C,D) only partially rescued the endocytic defects caused by either SNX18 or SNX9 depletion, suggesting that full-length SNX9 or SNX18 is required for complete rescue. This is conceivable considering that SNX18 and SNX9 are composed of four functional domains (SH3, LC, PX and BAR) that are known to bind a variety of proteins to regulate various steps of clathrin-mediated endocytosis (Lundmark and Carlsson, 2009; Shin et al., 2008).

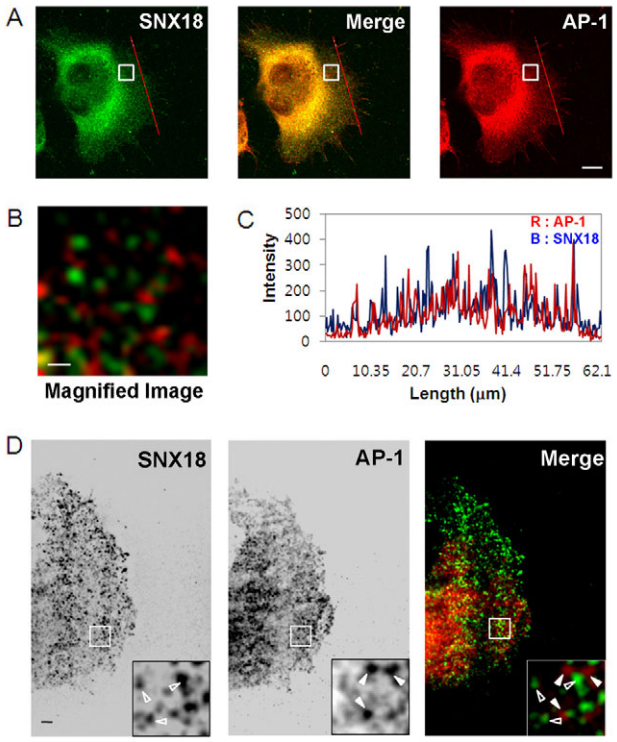

Fig. 5. SNX18 does not colocalize with AP-1. (**A-C**) Confocal micrographs of NIH3T3 cells co-stained for endogenous SNX18 and AP-1, and graph indicating the intensity profile of the red line in each image. AP-1 does not colocalize with SNX18. Scale bars: 10 μm (A), 1 μm (B). (**D**) TIRF microscopy images of NIH3T3 cells co-stained for endogenous SNX18 (left, green in merge) and AP-1 (middle, red in merge) show no colocalization (open arrowheads). Scale bar: 2 μm.

SNX18 is recruited to CCPs at a late stage

We next investigated the spatiotemporal dynamics of SNX18 in live cells and its association with CCP turnover using TIRF microscopy. The partial colocalization of SNX18 with CCPs reflects the transient interaction of SNX18 with CCPs (Fig. 6A). GFP-SNX18 and RFP-LCa (clathrin light chain) were transiently coexpressed in COS7 cells. Individual clathrin puncta appeared asynchronously, slowly increased in fluorescence intensity, plateaued and then rapidly disappeared. GFP-SNX18 colocalized as a transient burst with ~64% of the RFP-LCa spots, just before disappearance of the clathrin signal. Although there was some variability in the spatiotemporal relationship between SNX18 and clathrin, the peak of the SNX18 burst was observed to occur either just before or coincident with the disappearance of clathrin fluorescence from TIRF microscopy (Fig. 8A-C). The kinetics of the SNX18 burst were reminiscent of the transient recruitment of dynamin. Therefore, we examined the timing of SNX18 recruitment relative to dynamin-2. In most cases, 80% of the transient bursts of SNX18 colocalized with a burst of dynamin and the kinetics of changes in fluorescence intensity were indistinguishable (Fig. 8D,E). These results suggest that SNX18 and dynamin are transiently recruited to endocytic CCPs at a late stage of clathrin-coated vesicle formation. Consistent with our data suggesting that SNX9 and SNX18 dimerize, when co-transfected, the kinetics of GFP-SNX18 fluorescence and RFP-SNX9 fluorescence were indistinguishable; ~76% of the transient burst of SNX18 colocalized with a burst of SNX9 (Fig. 8F,G).

Discussion

SNX9 is now a well-understood protein that is required for clathrin-mediated endocytosis and clathrin-independent, actin-dependent fluid-phase endocytosis. SNX9 interacts with various proteins, such as dynamin, N-WASP, AP-2, Arp2/3 and PtdIns(4,5)P_2 kinases; these interactions are required for proper regulation of endocytosis (Shin et al., 2008). Vertebrate genomes express two proteins that are closely related to SNX9:

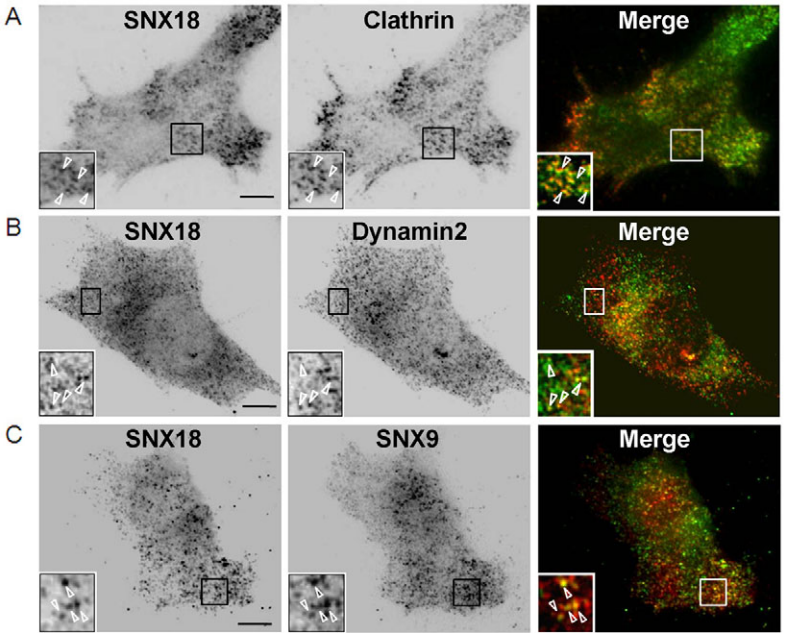

Fig. 6. SNX18 localizes at the cell surface, where it is partially colocalized with clathrin, dynamin and SNX9. TIRF microscopy images of NIH3T3 cells co-stained for endogenous SNX18 (left, green in merge) and clathrin (**A**), dynamin-2 (**B**) or SNX9 (**C**) (middle, red in merge) show partial but considerable colocalization in the vicinity of the plasma membrane (open arrowheads). Scale bars: 10 μm.

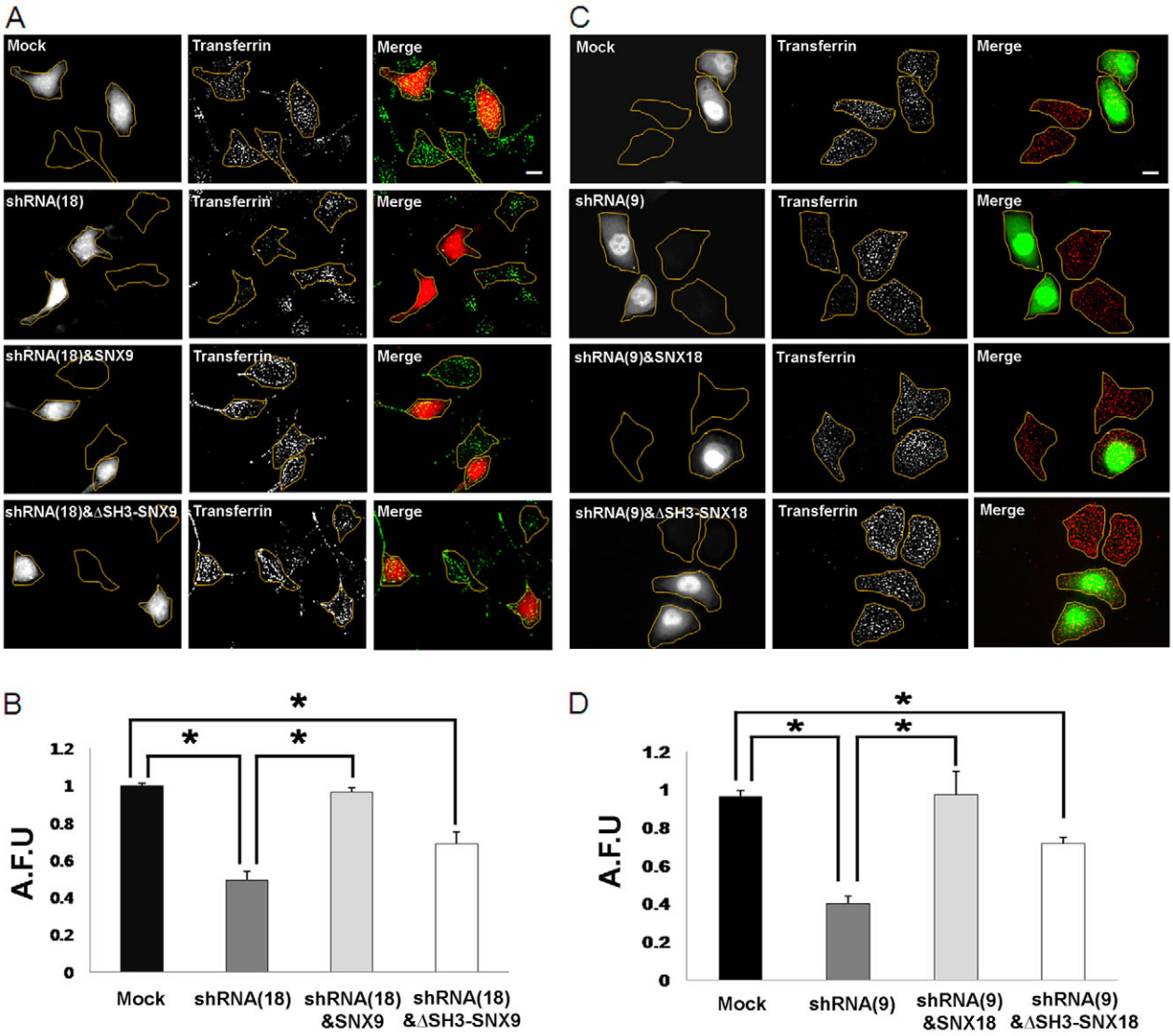

Fig. 7. SNX18 is required for transferrin uptake and compensates for the lack of SNX9 during clathrin-mediated endocytosis and vice versa. (**A**,**B**) C6 glioma cells were transfected with mock, shRNA-SNX18, shRNA-SNX18 plus SNX9 and shRNA-SNX18 plus ΔSH3-SNX9. Three days after transfection, cells were incubated with AlexaFluor488-transferrin for 10 minutes. After fixing, the cells were examined using microscopy. Cells were outlined for better comparison. Knock down of endogenous SNX18 reduced transferrin uptake by 55%. SNX9 fully rescued endocytic defects caused by SNX18 depletion in C6 glioma cells, whereas the SH3-deleted mutant of SNX9 did so partially. (**C**,**D**) HeLa cells were transfected with mock, shRNA-SNX9, shRNA-SNX9 plus SNX18 and shRNA-SNX9 plus ΔSH3-SNX18. Three days after transfection, cells were incubated with AlexaFluor488-transferrin for 10 minutes. Cells were outlined. Endocytic defects caused by SNX9 depletion in HeLa cells were fully rescued by SNX18 and partially rescued by SH3-deleted mutants of SNX18. These data demonstrate that SNX18 can replace the function of SNX9 in clathrin-mediated endocytosis and vice versa. Data are given as the mean ± s.e.; n=5. *Statistically significant at P<0.05, ANOVA and Tukey's HSD post hoc test for several different groups and Student's t-test for two different groups. Scale bar: 20 µm.

SNX18 and SNX33 (Haberg et al., 2008). These proteins constitute a separate subfamily of PX-BAR-containing SNX proteins. All three proteins contain similar domains: an N-terminal SH3 domain, LC and PX domains in the middle, and a C-terminal BAR domain (Haberg et al., 2008). They have ~40-70% sequence identity in the different domains, with the lowest identity found in LC domain. It seems that the ancestor of SNX18 and SNX33 branched off from SNX9 and was duplicated. *Caenorhabditis elegans* has only one ortholog of SNX9, SNX18 and SNX33, termed *lst-4* (Schobel et al., 2008). Overexpression of *lst-4* results in a phenotype very similar to a dynamin loss-of-function phenotype in *C. elegans*; this is consistent with previous results and our current results regarding the interaction of SNX9 and SNX18 with dynamin during endocytosis (Schobel et al., 2008).

Because SNX9 acts as a crucial regulator of vesicle trafficking, whether the three proteins have redundant roles or distinct roles in cells is of interest. Recent study showed that SNX33 binds dynamin and regulates amyloid precursor protein (APP) endocytosis in a dynamin-dependent manner. Also, SNX9 has a similar effect on APP shedding and APP cell-surface levels as SNX33, suggesting that they both function in endocytosis (Schobel et al., 2008). Another study showed that overexpression of SNX33 impaired cellular prion protein (PrPc) endocytosis at the plasma membrane, supporting the crucial role of SNX33 in endocytosis at the plasma

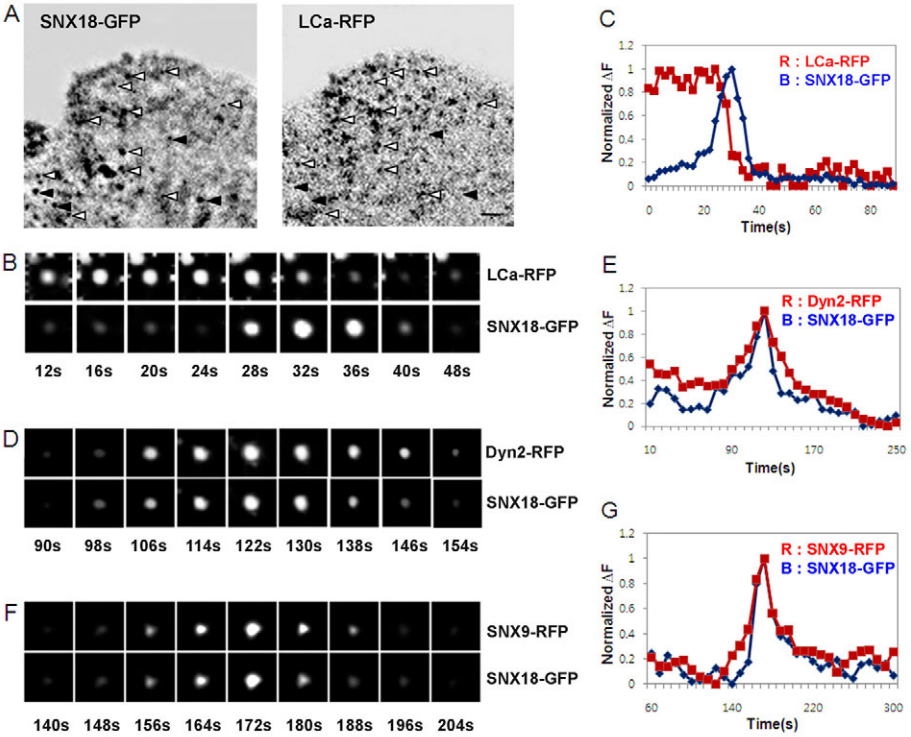

Fig. 8. SNX18 is recruited to CCPs at a late stage in vesicle formation. (**A**) TIRF microscopy images of a COS-7 cell co-transfected with SNX18-GFP and LCa-mRFP show colocalization (open arrowheads) or no colocalization (filled arrowheads). Scale bar: 2 µm. (**B**) Selected frames from a time-lapse sequence acquired every 2 seconds of a clathrin spot (top) and SNX18 spot (bottom). (**C**) Normalized fluorescence intensity changes as a function of time of a representative clathrin spot (red) and its corresponding 'burst' of SNX18 (blue). (**D-G**) Selected TIRF microscopy images from times series acquired every 2 seconds of dynamin-2 (D) or SNX9 (F), and SNX18. Normalized fluorescence graphs show spatial and temporal colocalization of SNX18 (blue) and dynamin-2 (E, red) or SNX9 (G, red).

membrane (Heiseke et al., 2008). A recent study, however, showed that SNX9, SNX18 and SNX33 localize differently and might function in different trafficking pathways. It was shown that SNX18 binds dynamin, but participates in membrane remodeling at endosomes together with AP-1 and PACS1, rather than functioning in endocytosis at the plasma membrane as SNX9 does, casting doubt on their suggested redundant roles (Haberg et al., 2008).

Our current results support the conclusion that SNX18 plays a role in endocytic pathways at the plasma membrane. Although we cannot completely rule out the possibility that these proteins have distinct roles, we believe that SNX18 is a redundant protein in the same pathways as SNX9, for the following reasons. First, most of the cell lines tested express SNX9 and SNX18, but to a different extent. In particular, SNX9 is highly expressed in HeLa and COS-7 cells, with quite low expression of SNX18, whereas the opposite is true in C6 glioma cells. Second, SNX18 interacts with dynamin, N-WASP and synaptojanin, well-known binding partners of SNX9. Third, knock down of SNX18 inhibits transferrin uptake. Furthermore, SNX18 successfully compensates for SNX9 deficiency during endocytosis and vice versa. Finally, in real-time TIRF imaging, exogenously expressed SNX9 and SNX18 showed a considerable amount of colocalization and their spatiotemporal movements are indistinguishable. All of the above results lead us to conclude that SNX18 functions in endocytosis, rather than in a distinct endosomal trafficking pathway. As discussed above, another member of the subfamily, SNX33, also functions in surface shedding and endocytosis of APP and PrPc. Therefore, we believe that SNX9, SNX18 and SNX33 function as regulators of endocytosis from the plasma membrane, although their cargos would depend mostly on their distributions.

Because SNX18 interacts with N-WASP, a regulator of the actin cytoskeleton, and actin, it raises the possibility that SNX18 has a role in actin-cytoskeleton-mediated endocytosis, such as fluid-phase endocytosis, as does SNX9 (Yarar et al., 2007). We could detect SNX18 in circular dorsal ruffles and membrane ruffles at the cell periphery of NIH3T3 cells after treatment with platelet-derived growth factor (PDGF). In addition, knock down of SNX18 markedly inhibited the uptake of Alexa594-labeled dextran (supplementary material Fig. S6). Therefore, whether SNX18 also regulates clathrin-independent fluid-phase endocytosis (as SNX9 does) is of interest.

A recent report showed that the brain is almost devoid of all three proteins. Previously, however, we showed that SNX9 is expressed in hippocampal neurons, where it has role in synaptic-vesicle endocytosis (Shin et al., 2007). Our in situ hybridization results showed that SNX18 is also highly expressed in the brain, especially the hippocampus and cerebellum. The recent study showed that SNX18 is enriched in dendritic spines (J.P. and S.C., unpublished results). SNX33 has roles in APP shedding and endocytosis, which should occur in brain regions (Schobel et al., 2008). Thus, unlikely previous reports, ours and other results suggest that all three proteins are expressed in brain regions and have roles in the nervous system. Although these different conclusions might arise from the different antibody sources or tissue preparations used, whether SNX18 and SNX33 act as regulators of synaptic-vesicle recycling, as SNX9 does, or whether they have discrete roles in the nervous system requires further investigation.

Materials and Methods

DNA constructs

SNX18, SNX9 and N-WASP were amplified by PCR and the PCR products were subcloned into pEGFP (Clontech, Mountain View, CA, USA), HA, Flag (modified from pEGFP-c1 vector), pTagRFP (Evrogen, Moscow, Russia) and pGEX-4T1 (Amersham Biosciences, Piscataway, NJ) vectors. The following constructs were PCR amplified and subcloned into expression vectors: SNX18-SH3 domain (residues 1-70), SNX18-ΔSH3 domain (residues 71-614), SNX18-BAR domain (residues 366-614), SNX18-ΔBAR domain (residues 1-385), SNX18-SH3LC domain (residues 1-265), SNX9-SH3 (residues 1-67), SNX9-ΔSH3 (residues 68-595) and SNX9-ΔBAR (residues 1-356). mRFP-Dyn2(baa) and LCa-mRFP were kindly provided by Pietro De Camilli (Yale University, New Haven, CT, USA). RFP-2xPH (FAPP1) and GFP-

2xFYVE (Hrs) were provided by Valker Haucke (Freie Universität Berlin, Berlin, Germany). All DNA constructs were verified by DNA sequencing.

Antibodies and reagents

The following antibodies were used. Anti-SNX18 rabbit polyclonal antibody was made by immunizing with GST-SH3-SNX18. Anti-SNX9 (Santa Cruz Biotechnology, Santa Cruz, CA), anti-dynamin-1 (ABR, Golden, CO, USA), anti-Hudy2 (Upstate Biotechnology, Lake Placid, NY, USA), anti-synaptojanin (Synaptic Systems, Göttingen, Germany), anti-GFP (Abcam, Cambridge, UK), anti-FLAG and anti-AP-1 (Sigma, St Louis, MO, USA), anti-N-WASP (Chemicon, Temecula, CA, USA), anti-HA (Covance, Princeton, NJ, USA), anti-CI-MPR (AbD Serotech, Oxford, UK) and anti-clathrin (Thermo Scientific, Rockford, IL, USA) were used. Secondary antibodies were obtained from Jackson ImmunoResearch (West Grove, PA, USA). AlexaFluor594-dextran, Texas Red-transferrin and AlexaFluor488-transferrin were from Molecular Probes (Eugene, OR, USA). PDGF-BB was from Calbiochem (San Diego, CA, USA) and all other reagents were from Sigma.

Cell culture, transfection and immunocytochemistry

All cell lines were cultured at 37°C and 5% CO_2 in DMEM (Invitrogen, San Diego, CA, USA) supplemented with 10% FBS (Hyclone, Logan, UT, USA). Transfection was carried out using Lipofectamine 2000 (Invitrogen) and cells were observed after 16-24 hours. For immunocytochemistry, cells were fixed in 4% formaldehyde, 4% sucrose, PBS for 15 minutes, permeabilized for 5 minutes in 0.25% Triton X-100, PBS and blocked for 30 minutes in 10% BSA, PBS at 37°C. The cells were incubated with primary antibodies, 3% BSA, PBS for 2 hours at 37°C or overnight at 4°C, washed in PBS, and incubated with secondary antibodies, 3% BSA, PBS for 45 minutes at 37°C.

Microscopy

Confocal images were acquired on an Olympus FV-1000 confocal microscope with a 60× 1.35 NA oil lens driven by FluoView 1000. Cells were excited with 488 nm (from an argon laser) and 559 nm light (from a diode laser). For TIRF microscopy, cells were imaged using an Olympus IX-71 microscope fitted with a 60× 1.45 NA TIRF lens and controlled by Cell^{M} software (Olympus). Laser lines (488 and 561 nm diode lasers) were coupled to the TIRF microscopy condenser through two independent optical fibers. The calculated evanescent depth was <150 nm. Cells were typically imaged in two channels by sequential excitation with 0.1 to 0.2 second exposures and detected with a back-illuminated Andor iXon 897 EMCCD camera (512 × 512, 16 bit; Andor Technologies, Belfast, Northern Ireland). The Image J program (National Institutes of Health) was used for analysis.

Protein knock down and transferrin uptake assay

shRNA for SNX9 (human) was described previously (Shin et al., 2008). SNX18 shRNA (rat) was designed from nucleotides 1239-1260. Complementary oligonucleotides were synthesized separately, with the addition of an *Apa*I site at the 5′ end and an *Eco*RI site at the 3′ end. The target sequence of shRNA was 5′-GAGGTGGAGAGCAAGATAGAT-3′. The annealed cDNA fragment was cloned into the *Apa*I-*Eco*RI sites of the pU6-mRFP vector (insert DsRed sequences to pSilencer.U.1.0 vector, Ambion). After transfection, the cells were incubated for 48 hours for immunoblotting and transferrin-uptake assay. The transferrin-uptake assay was carried out as previously described (Kim et al., 2006). Briefly, 3 days after transfection, cells were starved for 6-8 hours in serum-free DMEM with 0.1% BSA and incubated in serum-free DMEM-HEPES containing 20 μg/ml Alexa488-transferrin (Invitrogen) for 10 minutes at 37°C. Cells were washed in acid-stripping solution (150 mM NaCl, 2 mM $CaCl_2$ and 25 mM CH_3COONa, pH 4.5) and fixed in 4% paraformaldehyde. Fluorescent images were taken under a confocal microscope and analyzed using MetaMorph software (Molecular Devices, Downingtown, PA, USA). The outline of the cell shape was drawn in the DIC images and average fluorescence intensity per cell was measured. Then, the fluorescent intensity of transfected cells was normalized against that of non-transfected cells.

GST pull-down assays

The GST-SNX18-SH3, GST-SNX9-SH3 and GST-virgin vector plasmids were transformed into *Escherichia coli* BL-21. The transformants were cultured in 2XYT medium supplemented with ampicillin. After overnight induction with 0.5 mM isopropyl 1-thio-β-D-galactopyranoside at 25°C, the cultures were sonicated in lysis buffer [1% Triton X-100, 0.5% sodium deoxycholate, 20 mM Tris, pH 8.0, 150 mM NaCl, 1 mM $MgCl_2$, 1 mM EGTA, 0.1 mM phenylmethylsulphonyl fluoride (PMSF)] and centrifuged at 15,000 ***g*** for 15 minutes. The supernatants were incubated with glutathione-agarose-4B beads (Amersham Biosciences) at 4°C for 1 hour. After washing three times with lysis buffer, the beads were incubated at 4°C for 2 hours with brain lysates in lysis buffer. The beads were then washed extensively with lysis buffer and analyzed by SDS-PAGE and immunoblotting. To assess in vitro binding, the SNX9-His plasmid was transformed into *E. coli* BL-21. The transformants were cultured in 2XYT medium supplemented with ampicillin. After overnight induction with 0.5 mM isopropyl 1-thio-β-D-galactopyranoside at 25°C, the cultures were sonicated in NTA-lysis buffer (1% Triton X-100, 50 mM NaH_2PO_4, pH 8.0, 300 mM NaCl, 10 mM imidazole, 1 mM PMSF) and centrifuged at 15,000 ***g*** for 15 minutes. The supernatants were incubated with Ni-NTA chelating agarose CL-6B (Peptron Inc., Daejeon, Korea) at 4°C for 1 hour. After washing three times with NTA-washing buffer (0.1% Triton X-100, 50 mM NaH_2PO_4, pH 8.0, 300 mM NaCl, 20 mM imidazole, 1 mM PMSF), the beads were incubated at 4°C for 2 hours with NTA-elution buffer (0.1% Triton X-100, 50 mM NaH_2PO_4, pH 8.0, 300 mM NaCl, 300 mM imidazole). The eluted product was quantified by SDS-PAGE and subsequently used for in vitro binding experiments. SNX9-His was incubated at 4°C for 2 hours with purified GST or GST fusion proteins bound to glutathione beads in lysis buffer. The beads were then washed extensively and analyzed by SDS-PAGE and immunoblotting.

In-gel digestion and peptide sample preparation

The SDS-polyacrylamide gels were silver stained and protein bands were excised. The resulting samples were washed three times with a 1:1 (v/v) solution of acetonitrile and deionized water for 10 minutes, dehydrated with 100% acetonitrile, washed with a 1:1 (v/v) solution of 100% acetonitrile and 100 mM ammonium bicarbonate, and dried using a SpeedVac. They were then reduced with 10 mM tris(2-carboxyethyl)phosphine hydrochloride in 0.1 M ammonium bicarbonate at 56°C for 45 minutes and alkylated with 55 mM iodoacetamide in 0.1 M ammonium bicarbonate at room temperature for 30 minutes. The above washing step was repeated on the alkylated samples, which were dried, soaked in sequencing-grade trypsin solution (500 ng) on ice for 45 minutes, and immersed in 100 ml of 50 mM ammonium bicarbonate pH 8.0 at 37°C for 14-18 hours. The resulting peptides were extracted sequentially by agitation for 20 minutes with 45% acetonitrile in 20 mM ammonium bicarbonate, 45% acetonitrile in 0.5% trifluoroacetic acid, and 75% acetonitrile in 0.25% trifluoroacetic acid. The extracts containing tryptic peptides were pooled and evaporated under vacuum.

Micro-LC-MS/MS analysis and protein database search

In-gel digested proteins were loaded onto fused silica capillary columns (100 μm inner diameter, 360 μm outer diameter) containing 8 cm of 5 μm particle size Aqua C18 reverse-phase column material. The columns were placed in line with an Agilent HP 1100 quaternary LC pump and a splitter system was used to achieve a flow rate of 250 nl/minute. Buffer A (5% acetonitrile and 0.1% formic acid) and buffer B (80% acetonitrile and 0.1% formic acid) were used to make a 90 minute gradient. The gradient profile started with 5 minutes of 100% buffer A, followed by a 60 minute gradient from 0% to 55% buffer B, a 25 minute gradient from 55% to 100% buffer B, and a 5 minute gradient of 100% buffer B. Eluted peptides were directly electrosprayed into an LTQ linear ion trap mass spectrometer (ThermoFinnigan, Palo Alto, CA, USA) by applying 2.3 kV of DC voltage. Data-dependent scans consisting of one full MS scan (400-1400 m/z) and five data-dependent MS/MS scans were used to generate MS/MS spectra of the eluted peptides. Normalized collision energy of 35% was used throughout data acquisition. MS/MS spectra were searched against an NCBI rat protein sequence database using Bioworks version 3.1 and Sequest Cluster System (14 nodes). DTASelect was used to filter the search results and the following Xcorr values were applied to the different charge states of peptides: 1.8 for singly charged peptides, 2.2 for doubly charged peptides and 3.2 for triply charged peptides. Fragment ions in each MS/MS spectrum were manually assigned to confirm the database search results.

Coimmunoprecipitation and immunoblotting

To detect SNX18 and SNX9 binding to N-WASP in vivo, 293T cells were transfected with GFP, GFP-SNX18, GFP-SNX18-ΔSH3, GFP-SNX9 and GFP-SNX9-ΔSH3 together with HA-N-WASP using Liopofectamine 2000 (Invitrogen). The cells were washed twice with cold PBS and extracted at 4°C for 1 hour in a modified RIPA buffer (50 mM Tris-HCl pH 7.5, 5 mM EDTA, 150 mM NaCl, 1% Nonidet P-40, 1 mM sodium orthovanadate, 1 mM PMSF, 10 mM leupeptin, 1.5 mM pepstatin, and 1 mM aprotinin). They were then clarified by centrifugation at 15,000 ***g*** for 15 minutes and protein concentrations were determined with a Bradford protein assay reagent kit (Bio-Rad). Samples containing 1 mg of total protein were immunoprecipitated for 4 hours with anti-GFP antibody, followed by an additional 2 hours of incubation at 4°C with protein A-Sepharose beads (Amersham Biosciences). The immunoprecipitates were extensively washed with lysis buffer, subjected to SDS-PAGE and transferred to a polyvinylidine difluoride membrane (Bio-Rad). The membrane was blocked with 5% skim milk TBST (10 mM Tris-HCl, 100 mM NaCl and 0.1% Tween-10, pH 7.5) for 1 hour, washed and probed with primary antibody for 1 hour at room temperature. After extensive washing in TBST, the membrane was incubated with horseradish peroxidase (HRP)-conjugated secondary antibody (Jackson ImmunoResearch Laboratories). Proteins were visualized with enhanced chemiluminescence reagent (Amersham Biosciences). To examine homodimerization and heterodimerization of SNX18 and SNX9, 293T cells were transfected with various GFP-tagged SNX18 and SNX9 wild types and their mutants, together with FLAG-SNX18 using Lipofectamine 2000.

In situ hybridization

In situ hybridization on mouse E16, E18, P3, P7, P18 and adult brain sections was carried out with digoxigenin-labeled SNX18 RNA antisense probes and detected with anti-digoxigenin antibodies coupled to alkaline phosphatase (Roche Applied Biosystems, Pleasanton, CA, USA) and nitro blue tetrazolium-5-bromo-4-chloro-3-indolyl phosphate color substrate.

Native dynamin I purification and GTPase assay

Dynamin I was purified from mouse brain as described previously (Quan and Robinson, 2005). Briefly, amphiphysin-I-SH3-GST was immobilized on agarose beads and incubated with brain lysate for 2 hours. Bound dynamin I was eluted from amphiphysin-I-SH3-GST using a high salt elution buffer (1.2 M NaCl, 20 mM PIPES, 1 mM DTT, pH 6.5). The eluted dynamin I protein was placed in a diluting buffer (30 mM Tris/HCl, 100 mM NaCl pH 7.4) and quantified by SDS-PAGE. Dynamin I GTPase activity was measured using the GTPase Enzyme Linked Inorganic Phosphate Assay (ELIPA; Cytoskeleton Inc., Denver, CO, USA). Briefly, 1 μM dynamin I was mixed with 1 μM of SNX9 or SNX18. These protein mixtures were added to prepared ELIPA mixture with 1 mM GTP. A monochromatic spectrophotometer PowerWave XS (BioTek instruments, Winooski, VT, USA) was used to measure the amount of phosphate released by GTP hydrolysis and checked by absorbance at 360 nm using a kinetics assay with a 1 minute interval.

Dextran uptake

NIH cells were grown on coverslips at 37°C for 1 day and then transfected with SNX18-shRNA using Lipofectamine 2000 (Invitrogen). Two days after transfection, cells were incubated in the presence of 10 kDa AlexaFluor594-dextran (Invitrogen) with PDGF-BB (Calbiochem), fixed with 4% paraformaldehyde and mounted on coverslips. Fluorescence images were acquired on an Olympus IX-71 inverted microscope.

This research was supported by grants from the National Research Foundation of Korea (2009-0079446), the Brain Research Center of the 21st Century Frontier Research Program (M103KV010009-06K2201-00910), the National Core Research Center for Extreme Light Applications (to S.C.) and Korean Systems Biology Research (M10503010001-05N030100110) (to Z.Y.P.), funded by the Ministry of Education, Science and Technology, Republic of Korea. Confocal and TIRF microscopy data for this study were acquired and analyzed in the Biomedical Imaging Center at Seoul National University College of Medicine.

Supplementary material available online at
http://jcs.biologists.org/cgi/content/full/123/10/1742/DC1

References

Altschuler, Y., Barbas, S. M., Terlecky, L. J., Tang, K., Hardy, S., Mostov, K. E. and Schmid, S. L. (1998). Redundant and distinct functions for dynamin-1 and dynamin-2 isoforms. *J. Cell Biol.* **143**, 1871-1881.

Damke, H., Baba, T., Warnock, D. E. and Schmid, S. L. (1994). Induction of mutant dynamin specifically blocks endocytic coated vesicle formation. *J. Cell Biol.* **127**, 915-934.

Dawson, J. C., Legg, J. A. and Machesky, L. M. (2006). Bar domain proteins: a role in tubulation, scission and actin assembly in clathrin-mediated endocytosis. *Trends Cell. Biol.* **16**, 493-498.

Evergren, E., Gad, H., Walther, K., Sundborger, A., Tomilin, N. and Shupliakov, O. (2007). Intersectin is a negative regulator of dynamin recruitment to the synaptic endocytic zone in the central synapse. *J. Neurosci.* **27**, 379-390.

Farsad, K. and De Camilli, P. (2003). Mechanisms of membrane deformation. *Curr. Opin. Cell Biol.* **15**, 372-381.

Farsad, K., Ringstad, N., Takei, K., Floyd, S. R., Rose, K. and De Camilli, P. (2001). Generation of high curvature membranes mediated by direct endophilin bilayer interactions. *J. Cell Biol.* **155**, 193-200.

Gray, N. W., Fourgeaud, L., Huang, B., Chen, J., Cao, H., Oswald, B. J., Hemar, A. and McNiven, M. A. (2003). Dynamin 3 is a component of the postsynapse, where it interacts with mGluR5 and Homer. *Curr. Biol.* **13**, 510-515.

Haberg, K., Lundmark, R. and Carlsson, S. R. (2008). SNX18 is an SNX9 paralog that acts as a membrane tubulator in AP-1-positive endosomal trafficking. *J. Cell Sci.* **121**, 1495-1505.

Habermann, B. (2004). The BAR-domain family of proteins: a case of bending and binding? *EMBO Rep.* **5**, 250-255.

Heiseke, A., Schobel, S., Lichtenthaler, S. F., Vorberg, I., Groschup, M. H., Kretzschmar, H., Schatzl, H. M. and Nunziante, M. (2008). The novel sorting nexin SNX33 interferes with cellular PrP formation by modulation of PrP shedding. *Traffic* **9**, 1116-1129.

Hill, E., van der Kaay, J., Downes, C. P. and Smythe, E. (2001). The role of dynamin and its binding partners in coated pit invagination and scission. *J. Cell Biol.* **152**, 309-323.

Hinshaw, J. E. (2000). Dynamin and its role in membrane fission. *Annu. Rev. Cell Dev. Biol.* **16**, 483-519.

Itoh, T. and De Camilli, P. (2006). BAR, F-BAR (EFC) and ENTH/ANTH domains in the regulation of membrane-cytosol interfaces and membrane curvature. *Biochim. Biophys. Acta* **1761**, 897-912.

Itoh, T., Erdmann, K. S., Roux, A., Habermann, B., Werner, H. and De Camilli, P. (2005). Dynamin and the actin cytoskeleton cooperatively regulate plasma membrane invagination by BAR and F-BAR proteins. *Dev. Cell* **9**, 791-804.

Kim, S., Kim, H., Chang, B., Ahn, N., Hwang, S., Di Paolo, G. and Chang, S. (2006). Regulation of transferrin recycling kinetics by PtdIns[4,5]P2 availability. *FASEB J.* **20**, 2399-2401.

Kim, Y., Kim, S., Lee, S., Kim, S. H., Park, Z. Y., Song, W. K. and Chang, S. (2005). Interaction of SPIN90 with dynamin I and its participation in synaptic vesicle endocytosis. *J. Neurosci.* **25**, 9515-9523.

Klein, D. E., Lee, A., Frank, D. W., Marks, M. S. and Lemmon, M. A. (1998). The pleckstrin homology domains of dynamin isoforms require oligomerization for high affinity phosphoinositide binding. *J. Biol. Chem.* **273**, 27725-27733.

Lundmark, R. and Carlsson, S. R. (2002). The beta-appendages of the four adaptor-protein (AP) complexes: structure and binding properties, and identification of sorting nexin 9 as an accessory protein to AP-2. *Biochem. J.* **362**, 597-607.

Lundmark, R. and Carlsson, S. R. (2003). Sorting nexin 9 participates in clathrin-mediated endocytosis through interactions with the core components. *J. Biol. Chem.* **278**, 46772-46781.

Lundmark, R. and Carlsson, S. R. (2004). Regulated membrane recruitment of dynamin-2 mediated by sorting nexin 9. *J. Biol. Chem.* **279**, 42694-42702.

Lundmark, R. and Carlsson, S. R. (2009). SNX9- a prelude to vesicle release. *J. Cell Sci.* **122**, 5-11.

Masuda, M., Takeda, S., Sone, M., Ohki, T., Mori, H., Kamioka, Y. and Mochizuki, N. (2006). Endophilin BAR domain drives membrane curvature by two newly identified structure-based mechanisms. *EMBO J.* **25**, 2889-2897.

Nakata, T., Iwamoto, A., Noda, Y., Takemura, R., Yoshikura, H. and Hirokawa, N. (1991). Predominant and developmentally regulated expression of dynamin in neurons. *Neuron* **7**, 461-469.

Peter, B. J., Kent, H. M., Mills, I. G., Vallis, Y., Butler, P. J., Evans, P. R. and McMahon, H. T. (2004). BAR domains as sensors of membrane curvature: the amphiphysin BAR structure. *Science* **303**, 495-499.

Praefcke, G. J. and McMahon, H. T. (2004). The dynamin superfamily: universal membrane tubulation and fission molecules? *Nat. Rev. Mol. Cell. Biol.* **5**, 133-147.

Quan, A. and Robinson, P. J. (2005). Rapid purification of native dynamin I and colorimetric GTPase assay. *Methods Enzymol.* **404**, 556-569.

Roux, A., Uyhazi, K., Frost, A. and De Camilli, P. (2006). GTP-dependent twisting of dynamin implicates constriction and tension in membrane fission. *Nature* **441**, 528-531.

Schmid, E. M. and McMahon, H. T. (2007). Integrating molecular and network biology to decode endocytosis. *Nature* **448**, 883-888.

Schmid, E. M., Ford, M. G., Burtey, A., Praefcke, G. J., Peak-Chew, S. Y., Mills, I. G., Benmerah, A. and McMahon, H. T. (2006). Role of the AP2 beta-appendage hub in recruiting partners for clathrin-coated vesicle assembly. *PLoS Biol.* **4**, e262.

Schobel, S., Neumann, S., Hertweck, M., Dislich, B., Kuhn, P. H., Kremmer, E., Seed, B., Baumeister, R., Haass, C. and Lichtenthaler, S. F. (2008). A novel sorting nexin modulates endocytic trafficking and alpha-secretase cleavage of the amyloid precursor protein. *J. Biol. Chem.* **283**, 14257-14268.

Shin, N., Lee, S., Ahn, N., Kim, S. A., Ahn, S. G., YongPark, Z. and Chang, S. (2007). Sorting nexin 9 interacts with dynamin 1 and N-WASP and coordinates synaptic vesicle endocytosis. *J. Biol. Chem.* **282**, 28939-28950.

Shin, N., Ahn, N., Chang-Ileto, B., Park, J., Takei, K., Ahn, S. G., Kim, S. A., Di Paolo, G. and Chang, S. (2008). SNX9 regulates tubular invagination of the plasma membrane through interaction with actin cytoskeleton and dynamin 2. *J. Cell Sci.* **121**, 1252-1263.

Shpetner, H. S. and Vallee, R. B. (1989). Identification of dynamin, a novel mechanochemical enzyme that mediates interactions between microtubules. *Cell* **59**, 421-432.

Soulet, F., Yarar, D., Leonard, M. and Schmid, S. L. (2005). SNX9 regulates dynamin assembly and is required for efficient clathrin-mediated endocytosis. *Mol. Biol. Cell* **16**, 2058-2067.

Takei, K., Slepnev, V. I., Haucke, V. and De Camilli, P. (1999). Functional partnership between amphiphysin and dynamin in clathrin-mediated endocytosis. *Nat. Cell Biol.* **1**, 33-39.

Tsujita, K., Suetsugu, S., Sasaki, N., Furutani, M., Oikawa, T. and Takenawa, T. (2006). Coordination between the actin cytoskeleton and membrane deformation by a novel membrane tubulation domain of PCH proteins is involved in endocytosis. *J. Cell Biol.* **172**, 269-279.

Weissenhorn, W. (2005). Crystal structure of the endophilin-A1 BAR domain. *J. Mol. Biol.* **351**, 653-661.

Yarar, D., Waterman-Storer, C. M. and Schmid, S. L. (2007). SNX9 couples actin assembly to phosphoinositide signals and is required for membrane remodeling during endocytosis. *Dev. Cell* **13**, 43-56.

Yarar, D., Surka, M. C., Leonard, M. C. and Schmid, S. L. (2008). SNX9 activities are regulated by multiple phosphoinositides through both PX and BAR domains. *Traffic* **9**, 133-146.